ELSEVIER

Journal of Photochemistry and Photobiology A: Chemistry 120 (1999) 1–9

Journal of Photochemistry and Photobiology A:Chemistry

Translational motion and isomerization reaction near a solid–liquid interface studied by the interface sensitive transient grating method

Nobuhisa Nakajima, Noboru Hirota, Masahide Terazima*

Department of Chemistry, Graduate School of Science, Kyoto University, Kyoto 606, Japan

Received 30 April 1998; received in revised form 9 July 1998; accepted 1 October 1998

Abstract

Translational diffusion and *cis–trans* isomerization reaction of a liquid crystal molecule (N-(4-methoxybenzylidene)-4-*n*-butylaniline (MBBA)) at a solid–liquid interface were studied by the interface sensitive transient grating (TG) technique. The interface sensitivity was achieved by the total internal reflection for the probe light. In all solvents we used, the fringe length dependence of the decay rate constants of the species grating signal reveals that the diffusion constant at the interface region (49 nm) is similar to that in the bulk liquid. In some solvents, faster decays at interface than those in the bulk phase were observed, and they are mainly attributed to the enhanced *cis–trans* isomerization of MBBA at the interface. The enhancement is not sensitive to the solid surface conditions and depends on the solvents. These facts suggest that the enhancement originates from different solvent structures near the interface from those in the bulk phase. The isomerization rate measured in a porous glass was also increased from that in the bulk phase, which may support this suggestion. The interface sensitive TG signal of another photochromic molecule (spiropyran) was also detected.

Keywords: Translational motion; Isomerization reaction; Interface sensitive transient grating (TG) technique

1. Introduction

Recently, molecular dynamics at interfaces (solid–liquid, liquid–liquid, gas–liquid) attract much attention experimentally and theoretically because a large number of chemical or biological reactions occur at interfaces. Due to the importance, many experimental techniques have been developed to monitor the molecular structure, orientation and dynamics. [1–23] For example, orientation and orientational dynamics can be measured by the surface second harmonic generation [2–7] or sum frequency generation methods [8]. The molecular structure can be investigated by the infrared (IR) spectroscopy with the total internal reflection (TIR) [1] or Raman scattering technique [9].

Although reaction kinetics as well as the translational motion are very important for understanding reactions at interfaces, only a limited number of techniques have been developed. Diffusion of Brownian particles (latex suspension) close to a wall was studied by the light scattering technique with the TIR condition [10–12]. The correlation spectra were found to be very different from that in the bulk phase and completely interpreted in terms of the wall's reflection boundary [11]. One effect of the interface sensitive method is the fluorescence recovery method after a strong excitation by an optical interference pattern [15]. This technique is highly sensitive, but the applicability of this method is limited to fluorescent probe molecules. The method of probing the reaction kinetics is still undeveloped. It is required to develop another technique for fully understanding the molecular dynamics in the interface region.

The interface sensitive transient grating (TG) method, which does not require a fluorescent probe molecule but still has a high sensitivity can be another promising technique. A TG method with an evanescent wave for excitation and probe light was theoretically suggested to study the surface diffusion and photochemical reactions [24]. Independently we experimentally succeeded in detecting translational diffusion at a solid–liquid interface for the first time using the (nearly) uniform excitation along the normal to the interface and TIR for the probe light [25]. This condition may be appropriate for a simple analysis. We used the photoisomerization reaction of a liquid crystal, N-(4-methoxybenzylidene)-4-*n*-butylaniline (MBBA) as the probe molecule. The preliminary results showed that decay rates of the thermal grating and species grating signals were faster than those in the bulk phase. In this study, we extend this research to

*Corresponding author.

1010-6030/99/$ – see front matter
PII: S1010-6030(98)00415-8

clarify the translational diffusion and the isomerization kinetics near the interface quantitatively. A model calculation reveals that the faster decay of the species grating should be attributed to the enhanced back isomerization. The origin of the enhanced reaction near the interface is investigated by coating the solid surface and the solvent dependence of the rates. We suggest that the different solvent structure near the interface from that in the bulk phase is the origin of the enhancement of the back isomerization. The interface sensitive TG method of a photochromic molecule (Spiropyran) is also measured.

2. Experimental

The setup for the interface sensitive TG measurement was described elsewhere [25]. Briefly, the TG was created by the interference pattern between two excitation beams of the third harmonics of a Nd:YAG laser (Spectra-Physics GCR-170-10). The pump beams were introduced from upward to a sample, which is contained in a glass cell covered with a sapphire prism. The time dependence of the TG signal from the bulk phase (b-TG signal) was monitored by a probe beam from upward with an angle which satisfied the phase matching condition. The TG signal from the interface (i-TG signal) was monitored by another probe beam which was brought into the crossing region from the sapphire prism side under a TIR condition. These signals were detected by a photomultiplier tube. Temporal profiles of the signals were recorded by a digital oscilloscope (Tektronix 2430A) and averaged by a microcomputer.

The sample cell was made of a glass plate and a teflon sheet. The sapphire prism was washed with KOH aqueous solution at 50°C for 1 h and with nitric acid at 60°C. Finally, the prism was rinsed by 2-propanol before the experiment. For changing the surface condition, polystyrene was used to coat the sapphire surface. A diluted solution of the polymer was spread on the surface and rubbed by a paper. The thickness of the coated film was measured by an elipsometric method. The thickness was typically ∼14 nm.

A porous glass plate with a mean pore radius of 4 nm was purchased from Corning (Vycor, No. 7930). It was washed with nitric acid at 100°C for several hours, rinsed by distilled water and heated at 200°C for several days. MBBA and solvents were purchased from Tokyo Kasei Co. and Nacalai Tesque Inc., respectively. A typical concentration of MBBA was 0.4 M.

3. Analysis

In the TG experiment, molecules in solution are excited by the light with sinusoidally modulated intensity [25–30]. The fringe spacing Λ is given by $\lambda_{ex}/2 \sin(\theta/2)$ (λ_{ex}, wavelength of the excitation light and θ the crossing angle). By the nonradiative transition from the excited states, the thermal energy is released and it produces the thermal grating. If the photoexcited molecules are converted to another species, it creates the species grating. The TG signal is proportional to the square of the refractive index change by these processes:

$$I_{TG}(t) \propto \{\delta n_{th}(t) + \delta n_s(t)\}^2 \quad (1)$$

where δn_{th} and δn_s are the peak-null difference of the refractive index change by the thermal contribution and by the presence (or absence) of chemical species, respectively.

3.1. The TG signal from the bulk phase (b-TG signal)

For calculating the temporal profile of δn, thermal and mass diffusion equations should be solved with appropriate boundary and initial conditions. After impulsive heating and instantaneous chemical reactions such as *trans–cis* photoisomerization of MBBA (Scheme 1), the three-dimensional diffusion equations are given by

$$\frac{\partial \Delta \boldsymbol{T}}{\partial t} = \boldsymbol{D}_{th} \nabla^2 \Delta \boldsymbol{T} \quad (2)$$

$$\frac{\partial \Delta \boldsymbol{c}}{\partial t} = \boldsymbol{D}_c \nabla^2 \Delta \boldsymbol{c} - k_{ct} \Delta \boldsymbol{c} \quad (3)$$

$$\frac{\partial \Delta \boldsymbol{t}}{\partial t} = \boldsymbol{D}_t \nabla^2 \Delta \boldsymbol{t} + k_{ct} \Delta_t \quad (4)$$

where D_{th} is the thermal diffusion constant, D_c and D_t are the diffusion constants of the *cis* and the *trans* forms, ΔT is the temperature variation, Δc and Δt are the peak-null difference of the concentration of the *cis* and *trans* form, and k_{ct} is the rate constant of the *cis* to *trans* back isomerization in dark. The beam radius is assumed to be sufficiently large so that the thermal conduction and the mass diffusion across the excitation spot size can be neglected. Here we assume that the photoexcitation takes place uniformly along the optical

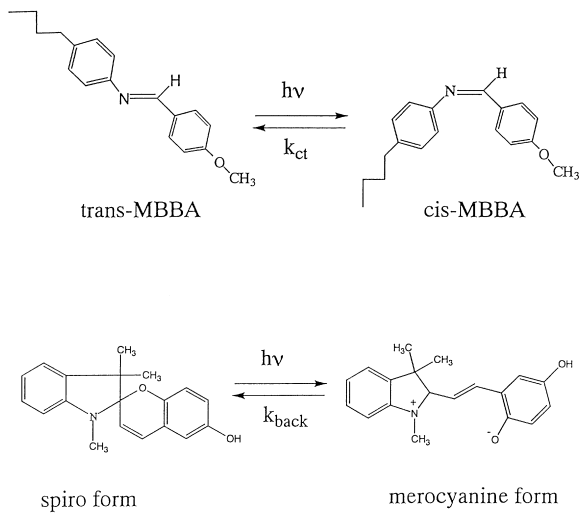

Scheme 1.

path (z-axis). Validity of this assumption will be considered later. The initial conditions are

$$\Delta T(x,y,z,t=0) = \frac{\Delta T_0[1-\cos(2\pi x/\Lambda)]}{2} \tag{5}$$

$$\Delta c(x,y,z,t=0) = \frac{\Delta c_0[1-\cos(2\pi x/\Lambda)]}{2} \tag{6}$$

$$\Delta t(x,y,z,t=0) = [t]_0 - \Delta c(x,y,z,t=0)$$

where Δc_0 is the initial concentration of the *cis* form prepared by photoexcitation and $[t]_0$ is the concentration of the *trans* form before irradiation.

For solving the differential equation for temperature, we assume an isotropic thermal diffusion constant. We further assume that D_c and D_t are also isotropic and the diffusion region is infinitely large. Under these assumptions, the diffusion equations (Eqs. (5) and (6)) can be simplified to be one-dimensional equations and can be solved simply as

$$\delta n_{th}(q,t) = \delta n_{th}^0 \exp(-D_{th}q^2 t)$$
$$\delta n_s(q,t) = \delta n_1 \exp(-D_t q^2 t) + \delta n_2 \exp\left[-(D_c q^2 + k_{ct})t\right] \tag{7}$$

where

$$\delta n_1 = \frac{-[\Delta c]\delta n_t (D_c q^2 - D_t q^2)}{D_c q^2 - D_t q^2 + k_{ct}}$$

$$\delta n_2 = [\Delta c]\left(\frac{\delta n_c - \delta n_t k_{ct}}{D_c q^2 - D_t q^2 + k_{ct}}\right)$$

and $q = 2\pi/\Lambda$. Hence, by plotting the decay rate constants of the species grating signal against q^2 (q^2 plot), D_{ct} as well as k_{ct} can be determined.

3.2. The TG signal from the interface region (i-TG signal)

For probing the molecular dynamics, we used (nearly) uniform excitation along to the optical path and TIR condition for the probe light, which provides a simple setup as well as a simple analysis. Under the TIR conditions for the probe light, an amplitude of the light decays exponentially in a direction normal to the interface plane (an evanescent wave), and the decay constant of the electric field amplitude (E) is called the penetration depth, d_p, which is given by [1]

$$E = E_0 \exp\left(\frac{-z}{d_p}\right)$$

$$d_p = \frac{\lambda_p}{2\pi n_1 \left(\sin^2\theta_i - (n_{21})^2\right)^{1/2}} \tag{8}$$

where λ_p is the wavelength of the probe light in vacuum, $n_{21} = n_2/n_1$ (n_1 and n_2; refractive indices in denser medium and that in rarer medium, respectively), and θ_i is the incident angle. If we assume that the refractive index of our sample is a volume-weighted average of the refractive indices of solvents and MBBA ($n = 1.38$), the penetration length d_p is obtained as 98 nm for ethanol solvent at 632.8 nm for the probe light under our experimental condition ($\theta_i = 76^\circ$ and $n = 1.77$ for sapphire [1]).

Since the probe beam is totally reflected at the interface, it will see an effective refractive index and diffracted by the spatially periodic variation of the refractive index. Neglecting a phase factor for the signal light, we obtain the TG signal intensity by

$$I_{TG}(t) \propto \left| E_0 e^{i\omega t} \int_0^\infty e^{-z/d_p}\, \delta n(t,z)\, dz \right|^2 \tag{9}$$

Considering that the TG signal intensity is proportional to the probe light intensity, we can monitor only the TG near the interface within half of the penetration depth ($d_p/2$), even though the TG is created through the whole sample thickness. Therefore, the TG signal under this experimental condition can monitor the averaged molecular dynamics from the interface to 49 nm region. Previously, a theoretical treatment of the TG diffraction efficiency under the reflection geometry was derived and it was used to investigate the thermal diffusion process at an interface [21–23]. Our study here is the first research for molecular diffusion process at the solid–liquid interface.

To calculate $\delta n(t,z)$, we use the diffusion equations (Eqs. (2)–(4)) and the initial conditions (Eqs. (5) and (6)). We assume that the sapphire prism is a semi-infinite half space heat sink with no thermal barrier at the interface, and the heat conduction in the sapphire is sufficiently fast. For the differential equation of the chemical species, the reflecting boundary condition is used, since the chemical species cannot penetrate into the solid prism. The differential equation is solved numerically based on the finite differential equation method (the Crank–Nicholson method) with 0.5 nm step [31].

4. Results and discussion

4.1. TG signal near the interface

After the photoexcitation of MBBA in ethanol, the TG signal from the bulk phase consists of two distinct signals [26,28]. One is the thermal grating signal by the heat releasing process from the excited states and the other is the species grating signal by the photoisomerization of MBBA from the trans form to the *cis* form (Scheme 1). Since there is no absorptive contribution from both species, the TG signal is proportional to the squire of the light induced change of the refractive index (δn). According to the analysis presented above, the temporal profile of the species grating signal can be expressed by a sum of two exponential functions (Eq. (7), [27]). However, in an isotropic phase, D of the *cis* form is nearly equal to the *trans* form ($D = D_c \approx D_t$) [26] and hence, the observed species grating signal can be reduced to a single exponential function as

$$I_{TG}(t)^{1/2} \propto \left|\delta n_s \exp\left[-(Dq^2 + k_{ct})t\right]\right| \quad (10)$$

where δn_s is the refractive index change by the presence (and absence) of the chemical species. In ethanol, it is known that the back isomerization reaction is slow compared with the period of the TG measurement (vide infra) and the plot of the decay rate constant against q^2 gives a straight line with a negligible intercept with the ordinate axis (Figure 4 in [25]).

The TG signal probed by the TIR light is very weak due to the very short interaction length ($d_p/2$). The excitation power should be increased compared with that for the bulk phase (the influence of the laser power will be discussed later) and the signal was averaged more than 600 shots. When the excitation laser was not so strong (vide infra), the qualitative features of the TG signal from the interface region of MBBA–ethanol (0.4 M) are similar to those from the bulk phase; the signal consists of the thermal and species grating components. However, quantitatively the temporal profile of the grating signal is different from that in the bulk liquid. In a previous paper [25], we reported the following observations for the i-TG signals after photoexcitation of MBBA in ethanol.

1. The decay rate of the thermal grating at the interface was much faster than that observed in the bulk phase. This feature can be reasonably reproduced by the thermal conduction from the liquid phase to the solid phase. The good agreement between the observed i-TG signal and the calculated one ensures that the observed signal actually monitors the dynamics at the interface.
2. The species grating signal at the interface was expressed well by a single exponential function and the lifetime was shorter than that in the bulk phase.

In the preliminary report [25], we inferred that the *cis–trans* back isomerization is enhanced at the interface from the q^2 dependence of the decay rate of the species grating. However, there are several factors which might affect the decay rate of the TG signal. We first examine these factors.

4.1.1. Excitation power

It is known that the time profile of the TG signal (in particular, from the liquid crystal sample) is distorted under a strong excitation laser power condition [28]. To ensure that the observed signal is not distorted by the excitation laser, we examine the laser power dependence of the TG signal. As described previously, the time profile of the species grating at sufficiently weak power can be expressed well with a single exponential function (Fig. 1(a)). However, when the excitation laser power is increased, a faster decaying component appears and a bi-exponential function is required to fit the profile (Fig. 1(b) and (c)).

$$I_{TG}(t) \propto |a_f \exp(-k_f t) + a_s \exp(-k_s t)| \quad (11)$$

where $k_s < k_f$ and $a_s a_f > 0$. When the distorted signal is fitted by the bi-exponential function, k_f is almost one order of magnitude larger than k_s and k_s is slightly smaller than the decay rate constant determined from the single exponential fitting in the lower power region. The decay rate constant in the lower region and k_s are plotted against the laser power in Fig. 2. The plot clearly shows that the lifetime of the TG signal within a weak laser power region does not depend on the laser power. Hence, we conclude that the observed i-TG signal does not suffer from the laser power shortening.

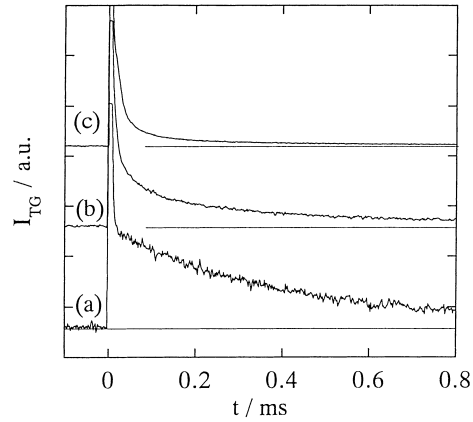

Fig. 1. The i-TG signal from MBBA/ethanol (0.4 M) under a weak (a) (2.5 μJ/cm^{-2}) and strong excitation conditions (b) and (c); (6.0 and 9.0 μJ/cm^{-2}, respectively). The signal intensity is normalized by the total species grating intensity.

4.1.2. Finite absorption length for excitation

Usually, the diffusion constant in the bulk phase has been measured under the weak absorption condition by the TG method; that is, the photoexcitation takes place uniformly through the sample thickness or the crossing region of the two excitation beams. However, in this i-TG case, the absorption length for the excitation light has to be short to improve the S/N ratio. The extinction coefficient of MBBA in ethanol at 355 nm is measured to be

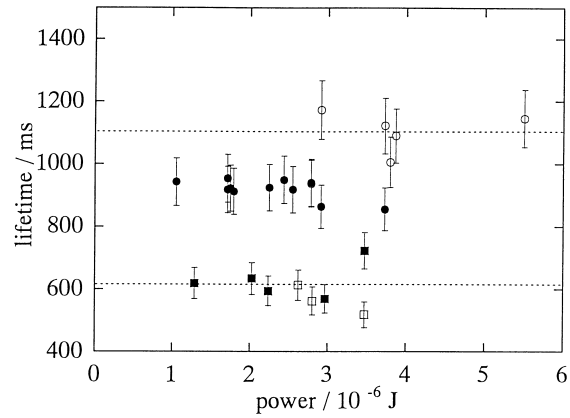

Fig. 2. Laser power dependence of the lifetime of the i-TG signal in ethanol (circles) and acetonitrile (squares) as example. Closed and open symbols denote the rate constants determined by the single and double exponential fitting, respectively. Upper and lower dotted lines represent the lifetime in the bulk phase of ethanol and acetonitrile solvents, respectively.

$7 \times 10^3\ \mathrm{M^{-1}\,cm^{-1}}$. For the 0.4 M solution, the absorption length is $d_a = 3.6\,\mu\mathrm{m}$. If the fringe spacing is shorter than this length, the sinusoidal modulation of the concentration along the grating vector will be completely averaged before the effect of the finite absorption length appears. On the other hand, if the fringe spacing is not short enough, the diffusion to the z-axis will change the time profile from what is expected by the one-dimensional diffusion (Section 3).

This effect is examined by a numerical calculation. The initial condition of Eqs. (5) and (6) is modified to

$$\Delta c(x, y, z, t = 0) = \frac{\Delta c_0 \exp(-z/d_a)[1 - \cos(2\pi x/\Lambda)]}{2} \tag{12}$$

to take into account the finite absorption length (d_a). At various d_a, the i-TG signals are calculated and presented in Fig. 3. When d_a becomes close to Λ, the i-TG signal decays faster initially. This faster decay can be understood in terms of the additional diffusion path to the z-axis. However, after a short time (such as 20 μs in Fig. 3), the signal decays exponentially. The lifetime of the single exponential part agrees with that of the uniform excitation case within 1% even if $d_a = \Lambda/5$. Hence as long as the initial part is disregarded (which is inevitable because of the disturbance from the strong thermal grating signal), the lifetime of the i-TG should not be affected by the finite absorption length.

4.1.3. Contribution of aggregate

Since the concentration of MBBA should be high (0.4 M) to improve the S/N ratio, the solute could form aggregates, which might contribute to the TG signal. However, we found that D obtained from the b-TG signal of 0.4 M solution is close to that of 1 mM solution after a correction of the viscosity change. Hence, we conclude that the contribution of aggregates to the TG signal is minor even it is exists.

4.2. Analysis of the i-TG signal

In our previous paper,[25] we analyzed the i-TG signal by the single exponential fit and the decay rate was plotted against q^2. However, if D or k_{ct} are not uniform in the diffusing space, the signal may not decay exponentially. In order to examine the validity of this exponential fitting, we calculate the temporal profile of the species grating signal by solving the differential equations (Eqs. (5) and (6)). For simplicity, we assume that D along the x-axis (D_x) is an exponential function of only the distance from the interface. The rate constant for the back isomerization k_{ct} is also assumed to be an exponential function from the interface.

$$D_x(z) = D_x^{\mathrm{b}} + (D_x^{\mathrm{i}} - D_x^{\mathrm{b}}) \exp\left(\frac{-z}{d_{\mathrm{d}}}\right) \tag{13}$$

$$k_{\mathrm{ct}}(z) = k_{\mathrm{ct}}^{\mathrm{b}} + \left(k_{\mathrm{ct}}^{\mathrm{i}} - k_{\mathrm{ct}}^{\mathrm{b}}\right) \exp\left(\frac{-z}{d_{\mathrm{k}}}\right) \tag{14}$$

where superscripts i and b stand for the bulk liquid and the interface, respectively, d_d (d_k) is a characteristic length for describing the diffusion constant (rate constant of the back isomerization).

Here we consider two cases.

Case 1. Diffusion constant near the interface is faster than in the bulk region ($D_x^{\mathrm{i}} > D_x^{\mathrm{b}}$) but the isomerization rate does not depend on z ($k_{\mathrm{ct}}^{\mathrm{i}} = k_{\mathrm{ct}}^{\mathrm{b}}$).

Case 2. Back isomerization near the interface is enhanced ($k_{\mathrm{ct}}^{\mathrm{i}} > k_{\mathrm{ct}}^{\mathrm{b}}$) with $D_x^{\mathrm{i}} = D_x^{\mathrm{b}}$.

Fig. 4(a) shows typical examples of the time profile of the i-TG signals calculated with parameters. (Case 1: $D_x^{\mathrm{b}} = 0.47 \times 10^{-9}\ \mathrm{m^2/s}$ (diffusion constant of MBBA in ethanol (0.4 M solution)), $D_x^{\mathrm{i}} = 4.7 \times 10^{-9}\ \mathrm{m^2/s}$, $d_{\mathrm{d}} = 2\ \mathrm{nm}$, $k_{\mathrm{ct}}^{\mathrm{b}} = k_{\mathrm{ct}}^{\mathrm{i}} = 1\ \mathrm{s^{-1}}$. (Case 2): $D_x^{\mathrm{b}} = D_x^{\mathrm{i}} = 0.47 \times 10^{-9}\ \mathrm{m^2/s}$, $k_{\mathrm{ct}}^{\mathrm{b}} = 1\ \mathrm{s^{-1}}$, $k_{\mathrm{ct}}^{\mathrm{i}} = 5 \times 10^3\ \mathrm{s^{-1}}$, and $d_{\mathrm{k}} = 2\ \mathrm{nm}$. Both i-TG signals can be well expressed by a single exponential function.

When the decay rates at various q^2 are plotted against q^2 (q^2 plot) (Fig. 4(b)), it is apparent that the rate constants are proportional to the q^2 values. Case 1 shows a larger slope with a small intercept at $q^2 = 0$ axis, while the plot of Case 2 has very similar slope as $D_x^{\mathrm{b}} q^2$ with a finite intercept with the $q^2 = 0$ axis. These features are similar to what are expected for the b-TG signal. It should be noted that the slope in Case 1 represents the effective D averaged over d_p region. Hence the apparent D (D_{app}) in this case is close to $D^{\mathrm{b}}(1 - d_{\mathrm{d}}/d_{\mathrm{p}}) + D^{\mathrm{i}}(d_{\mathrm{d}}/d_{\mathrm{p}})$. Similarly, the apparent rate constant (k_{app}) in Case 2 is close to $k_{\mathrm{ct}}^{\mathrm{b}}(1 - d_{\mathrm{k}}/d_{\mathrm{p}}) + k_{\mathrm{ct}}^{\mathrm{i}}(d_{\mathrm{k}}/d_{\mathrm{p}})$. These model calculations justify our exponential fitting of the i-TG signal and the q^2 plot. Based on these results, the q^2 plot of the i-TG signal implies $D^{\mathrm{i}}(d_{\mathrm{d}}/d_{\mathrm{p}}) \sim 0$ and $k_{\mathrm{ct}}^{\mathrm{i}}(d_{\mathrm{k}}/d_{\mathrm{p}}) \sim 0.3\ \mathrm{ms^{-1}}$ for the ethanol solvent.

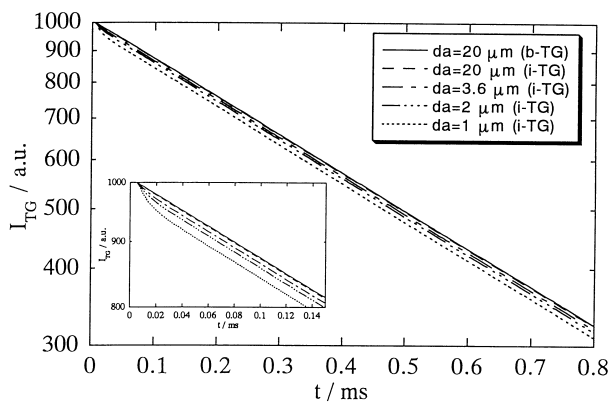

Fig. 3. Calculated b-TG and i-TG and i-TG signals at various absorption lengths (d_a for $q^2 = 1.5 \times 10^{12}\ \mathrm{m^{-2}}$ ($\Lambda = 5.1\ \mu\mathrm{m}$).

4.3. Origin of the enhanced isomerization

As shown in the previous section, the shorter lifetime of the i-TG signal can be interpreted in terms of the enhanced isomerization reaction near the interface. There may be two possible origins to account for this enhancement.

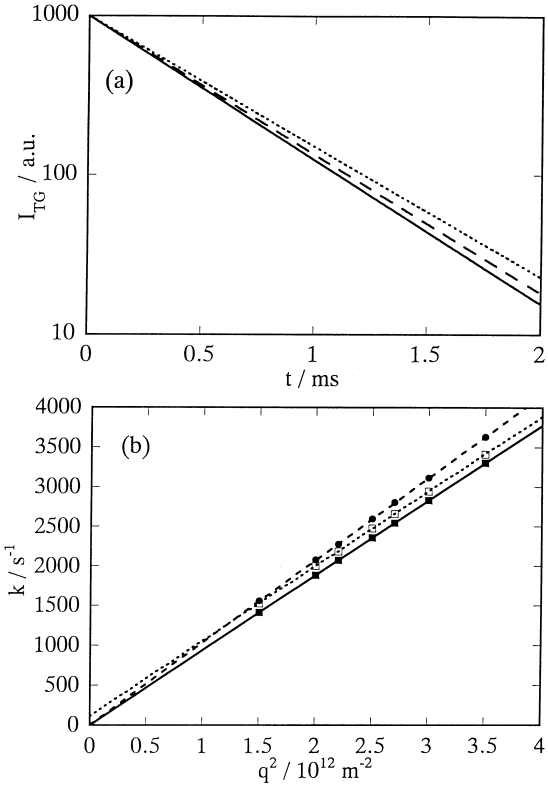

Fig. 4. (a) Calculated i-TG signals with parameters (solid line; for the bulk phase of ethanol) $D_x^b = D_x^i = 0.47 \times 10^{-9}$ m^2/s, $k_{ct}^b = k_{ct}^i = 1$ s^{-1} (broken line; for Case 1), $D_x^b = 0.47 \times 10^{-9}$ m^2/s, $D_x^i = 4.7 \times 10^{-9}$ m^2/s, $d_d = 2$ nm, $k_{ct}^b = k_{ct}^i = 1$ s^{-1}, and (dotted line for Case 2) $D_x^b = D_x^i = 0.47 \times 10^{-9}$ m^2/s, $k_{ct}^b = 1$ s^{-1}, $k_{ct}^i = 5 \times 10^3$ s^{-1}, and $d_k = 2$ nm. (b) q^2 plot of the calculated i-TG signal for the above parameters (Closed squares; for bulk, closed circles; for Case 1, open squares; for Case 2). The lines are fitted lines by the least square method.

1. The surface of the sapphire prism may act as a catalyst to the back reaction.
2. The solvent structure near the interface is different from that in the bulk phase and it enhances the back reaction.

These two possibilities were examined by coating the sapphire surface and by the solvent dependence.

4.3.1. Polymer coating

The surface of the sapphire prism was coated by a polystyrene film. The thermal i-TG from the coated sample cell was almost identical to the i-TG signal without the coating, which indicates that the thermal conduction to the solid phase determine the decay of the signal. The lifetime of the species grating was also the same within our experimental uncertainty (±10%) and it was shorter than that of the b-TG signal. This result implies that the back isomerization is enhanced regardless of the surface condition, either sapphire or polystyrene. Disregarding that the accidental coincidence of the catalytic capabilities of these surfaces, we think that the enhancement is not due to the surface catalytic reaction.

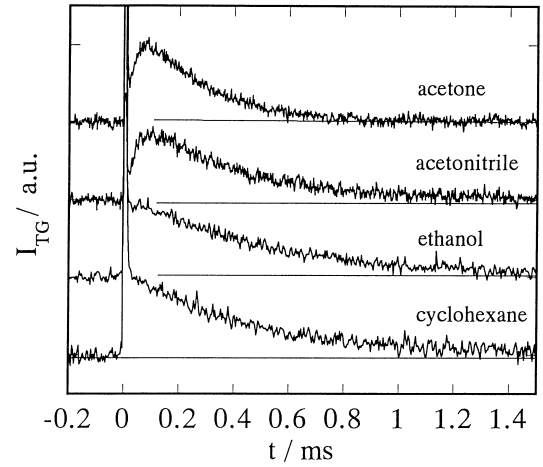

Fig. 5. The i-TG signal in various solvents.

4.3.2. Solvent dependence

We measured the i-TG signal in various solvents such as ethanol, methanol, acetonitrile, acetone, benzene, hexane, and cyclohexane. Since the refractive index of these solvents are not so much different, half of the penetration length calculated from Eq. (8) are almost constant around 50 ± 3 nm except benzene ($d_p/2 = 58$ nm). In fact, the thermal grating signal from the interface is very similar to each other in every solvent, which is a clear indication that the signal comes from very similar interface region. The time profile of the i-TG signal in ethanol, benzene and cyclohexane can be fitted well by a single exponential function, while those in acetonitrile, hexane, methanol and acetone show slow rising component (Fig. 5). In these solvents, the time profile was fitted by a sum of two exponential functions with pre-exponential factors of different sign. Under the same condition, the b-TG signal decays single exponentially in every solvent. (A deviation from a single exponential decay was observed for the i-TG signal even in ethanol, when we used more concentrated solution. In this case, however, a faster decay component appears. These slow rise or faster decay might result from an intermolecular interaction between MBBA at the solid–liquid interface. We could not check whether the slow rising component disappears or not under more diluted condition of acetonitrile, hexane, methanol and acetone, because of the weaker signal intensity.) At present, we do not understand what caused the slow rising component. However, since the decay lifetime is close to Dq^2, it is sure, at least, that the i-TG decays represent the diffusion process of MBBA in these solvents. The excitation power dependence of the lifetime in all solvents is checked to find that the lifetimes are constant within the experimental error in every solvent (an example is shown in Fig. 2). The decay rates were plotted against q^2, and two typical examples are shown in Fig. 6. We found that the i-TG signals in ethanol, methanol, benzene, and cyclohexane decay faster than the b-TG signal and show non-

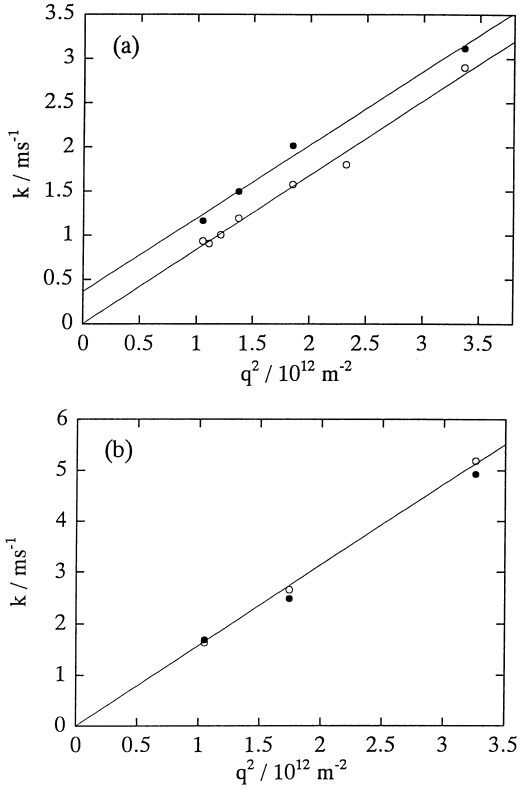

Fig. 6. Two typical examples of the q^2 plots of the decay rates from the i-TG signals (closed circles) and from the b-TG signal (open circles) in (a) cyclohexane and (b) acetonitrile.

negligible intercepts to $q^2 = 0$ axis. On the other hand, in acetonitrile, hexane, and acetone, the decay rates were very similar to that of the b-TG signal at any q^2, therefore, D and k_{ct}^{i} should be similar to those in the bulk phase, too. This solvent dependence indicates that the enhanced isomerization is related with the nature of the solvent.

Since an isomerization reaction requires a space which allows the bulky group to move, it is expected that the *cis–trans* isomerization rate depends on the free space of the solvent [32]. A medium with a larger free space will increase the isomerization rate. The enhanced back reaction near the interface may be explained by the larger free space near the interface. Due to the intermolecular interaction, the solvent molecules have intermolecular local structures. This local structure may be broken near the solid wall and it may create a large free space than in the bulk phase, which will increase the isomerization reaction. A molecular dynamics simulation of organic solutions near solid interfaces indicates some ordered structures close to the wall [14,17]. The ordering is destroyed around 0∼2 nm region from the surface and the structures near solid surfaces are different from that in the bulk phase. This transient spatial disordering may relate to the larger free space.

In order to reduce the fitting error of the q^2 plot, D_{app} in every solvent is assumed to be the same as D^b to determine the intercept at $q^2 = 0$ (i.e., $k_{app} = k_{ct}^{b}(1 - d_k/d_p) + k_{ct}^{i}(d_k/d_p)$). The solvent dependence of k_{app} can be explained either

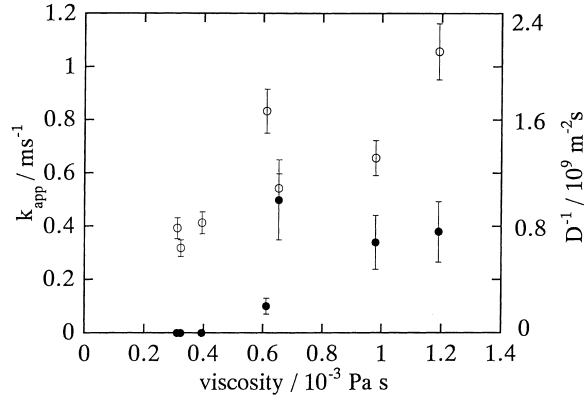

Fig. 7. The inverse of D (open circles) and the *cis–trans* isomerization rates (k_{ct}) (closed circles) determined from the q^2 plots against the solvent viscosity.

by the different free volume near the interface (different k_{ct}^{i}) or different d_k. We tried to seek solvent properties (such as dielectric constant, capability of the hydrogen bonding etc.) which correlate with the enhancement of the isomerization and found that the enhanced isomerization rate near the interface is more pronounced in a solvent with a higher viscosity. In Fig. 7, D^{-1} and k_{app} determined from the q^2 plot are shown. D^{-1} is proportional to the viscosity as expected from the Stokes–Einstein relation ($D^{-1} = ar\eta/kT$: a, constant; r, radius of the solute; η, viscosity; T, temperature). The viscosity dependence of k_{app} is less obvious in Fig. 7 but it increases with increasing the viscosity (except in benzene ($\eta = 0.65$ mPa s)). This viscosity dependence can be related to the above free space model. The viscosity is approximately related with the intermolecular interaction for small nonassociated solvents. The above finding may suggest that the strongly interacting solvents could have a larger interface region for the free space (d_k) and, hence, k_{app} is expected to be larger. The larger k_{app} in benzene might reflect the strong intermolecular interaction of benzene, which induces a more pronounced local structure as observed experimentally [33].

4.3.3. Isomerization in the porous glass

In principle, the back isomerization rate in the bulk phase can be determined for the q^2 plot of the decay rate of the i-TG signal (Eq. (10)). However, since the value of the intercept to the vertical axis at $q^2 = 0$ is very small compared with the decay rate, k_{ct} from the q^2 plot is not accurate. The lifetime of the *cis* isomer in the bulk phase was measured by the laser photolysis method. Monitoring a probe light intensity at 360 nm, we observed the transient bleach signal after the photoirradiation. This bleach signal indicates that the extinction coefficient of the *cis* isomer is much smaller than that of the *trans* isomer at this wavelength. The bleach recovery rate should represent the *cis*-to-*trans* isomerization. The lifetime of *cis*-MBBA in ethanol is 1.4 s (Fig. 8).

By the same method, we tried to detect the bleach signal from the sapphire–ethanol interface, but the signal was very

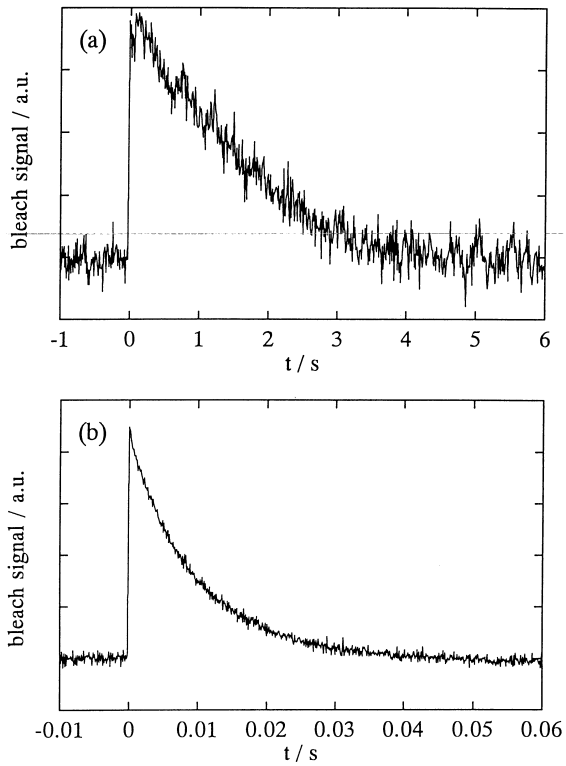

Fig. 8. Transient bleach signals of MBBA in ethanol (a) in the bulk and (b) in the porous glass.

weak due to that short penetration length. We used a porous glass to measure the lifetime of the *cis* isomer close to the solid surface directly by the transient absorption method.

A porous glass is an interesting media, in which many molecular dynamics have been measured [34–36]. In one of related studies, Dozier et al. have measured the self-diffusion of azobenzene is solution in porous glass by the TG method [34]. They found that azobenzene in a porous glass without treatment by 1-propanol showed a q-independent decay, which could be due to enhanced isomerization of azobenzene adsorbed to the pore surface. When the porous glass was treated by 1-propanol at its boiling temperature, the active site of the glass was blocked and they did not find any q-independent decay. In order to avoid this possible additional isomerization process, we have treated our porous glass by the same method to block the active site for adsorption before our measurements.

The bleach signal from MBBA in a porous glass is shown in Fig. 8. The lifetime (∼8 ms) is dramatically shortened in the porous glass compared with that in the bulk phase (1.2 s). The short lifetime *cis*-MBBA is consistent with the results of the interface sensitive TG experiments. The enhanced isomerization may be induced by a special intermolecular structure in the pore.

4.4. The i-TG signal of spiropyrane

Using the photoisomerization reaction of MBBA, we found that D near the interface is very close to D in the bulk. We used another reaction to investigate D under the TIR probe condition. A spiropyran (1′,3′,3′-trimethyl-6-hydroxyspiro(2H-1-benzopyran-2′,2′-benzopyran-2′,2′-indoline)) is a well known photochromic molecule (Scheme 1). [37–39] On UV photoexcitation, it is converted to a colored mecrocyanine form and it is thermally converted back to the original form gradually. This photochromic reaction induces strong species grating signal under the TG excitation condition [37]. Fig. 9 depicts the species grating signal of b-TG and i-TG signals in hexanol. Both signals can be expressed well with a single exponential function and the lifetimes were the same within our experimental uncertainty (±5%). The same lifetime indicates that D as well as k_{back} near the solid–liquid interface are close to those in the bulk phase for this molecule.

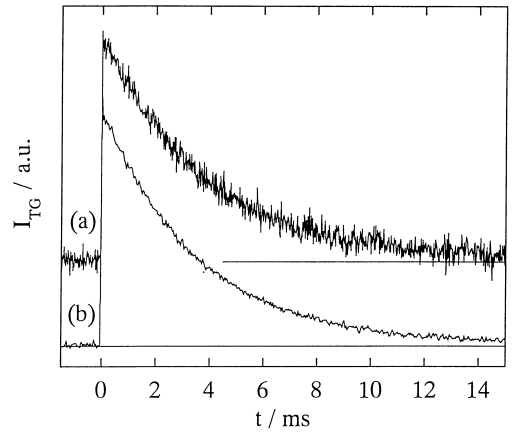

Fig. 9. The TG signals after photoexcitation of a spiropyran in hexanol (a) in the bulk phase (b-TG) and (b) under the TIR probe condition (i-TG).

4.5. Translational diffusion at the solid–liquid interface

Diffusion could be slowed down at a position very close to a wall due to the wall-molecular interaction (drag effect). The effect of the trapping layer will be penetrated in the fluid phase by the intermolecular interaction. From NMR measurements of water in porous silica glass, it was found that water molecules below one monolayer are less mobile by the liquid–solid interaction [36]. Molecular dynamics simulation of alkanes on a solid surface showed that apparent diffusion constant along the z direction (normal to the surface) decreases near the surface, which may result from the effect of the reflecting surface. On the other hand, parallel to the surface is enhanced near the surface because of the flat and smooth structure of the surface [14]. This anomaly of D near the interface was not detected by the TG technique with the TIR probing method probably because of the relatively long penetration depth compared with d_d ($d_d/d_p < 1$). (For isomerization reaction rate, we think that d_k should be similar to d_d (i.e., $d_k/d_p < 1$). However, in this case, since k_{ct}^i is much larger than k_{ct}^b (Section 4.3.3), k_{app} becomes larger than k_{ct}^b beyond the experimental uncertainty in some solvents.)

From an evanescent light propagation in the nematic liquid crystal, the motion near a rubbed nylon surface was found to be slower than in the bulk phase and the surface anchoring energy was evaluated from the surface correlation function of the liquid crystal sample [12]. This observation, slow motion at the interface by the TIR probing, may result from a long correlation length in the nematic phase due to the strong intermolecular interaction. However, our preliminary measurement of the i-TG method of MBBA nematic phase reveals that the diffusion near the interface is very similar to that in the bulk phase even in the nematic phase. We are now investigating the molecular dynamics near the interface of a nematic liquid crystal in detail as well as near the other interfacial regions such as the gas–liquid or liquid–liquid interfaces.

5. Summary

Molecular dynamics after photoexcitation of a liquid crystal molecular (MBBA) at a solid–liquid interface was studied by the TG method with TIR for the probe light. In ethanol, methanol, benzene and cyclohexane, the species grating signal from the interface region decays faster than that from the bulk phase, while the difference is much smaller in acetonitrile, hexane and acetone. The faster decay was attributed to the enhanced back isomerization reaction of MBBA near the surface. The solvent dependence indicate that the enhanced isomerization is originated from a different solvent structure near the interface from that in the bulk phase. The diffusion constant in all solvents near the interface (50 nm) was very similar to those in the bulk phase. The similarity was also confirmed by the i-TG signal from another solute (spiropyran).

References

[1] N.J. Harrick, Internal Reflection Spectroscopy, Interscience, New York, 1967.
[2] E.V. Sitzmann, K.B. Eisenthal, J. Chem. Phys. 90 (1989) 2831.
[3] A. Castro, E.V. Sitzmann, D. Zhang, K.B. Eisenthal, J. Phys. Chem. 95 (1991) 6752.
[4] K.B. Eisenthal, Annu. Rev. Phys. Chem. 43 (1992) 627.
[5] K.B. Eisenthal, Chem. Rev. 96 (1996) 1343.
[6] X. Zhao, M.C. Goh, S. Subrahmanyan, K.B. Eisenthal, J. Phys. Chem. 94 (1990) 3370.
[7] S.R. Meech, K. Yoshihara, Chem. Phys. Lett. 174 (1990) 423.
[8] P. Guyot-Sionnest, R. Superfine, J.H. Hunt, Y.R. Shen, Chem. Phys. Lett. 144 (1988) 1.
[9] B. Yahiaoui, M. Masson, M. Harrand, J. Chem. Phys. 93 (1990) 6047.
[10] R. Steininger, J. Bilgram, Helv. Phys. Acta 62 (1989) 215.
[11] K.H. Lan, N. Ostrowsky, D. Sornette, Phys. Rev. Lett. 57 (1986) 17.
[12] C.S. Park, M. Copic, R. Mahmood, N.A. Clark, Liq. Cryst. 16 (1994) 135.
[13] A.L. Wong, J.M. Harris, J. Phys. Chem. 95 (1991) 5895.
[14] R.G. Winkler, T. Matsuda, D.Y. Yoon, J. Chem. Phys. 98 (1993) 729.
[15] S.L. Zulli, J.M. Kovaleski, X.R. Zhu, J.M. Harris, M.J. Wirth, Anal. Chem. 66 (1994) 1708.
[16] X.-Y. Liu, P. Bennema, L.A. Meijer, M.S. Couto, Chem. Phys. Lett. 220 (1994) 53.
[17] P.G. Winkler, R. Hentschke, J. Chem. Phys. 100 (1994) 3930.
[18] M. Toriumi, H. Masuhara, Spectrochim. Acta 14 (1991) 353.
[19] S. Hamai, N. Tamai, H. Masuhara, Chem. Phys. Lett. 213 (1993) 407.
[20] S. Hamai, N. Tamai, H. Masuhara, J. Phys. Chem. 99 (1995) 4980.
[21] I.M. Fishman, C.D. Marshall, J.S. Meth, M.D. Fayer, J. Opt. Soc. Am. B8 (1991) 1880.
[22] I.M. Fishman, C.D. Marshall, A. Tokmakoff, M.D. Fayer, J. Opt. Soc. Am. B10 (1993) 1006.
[23] C.D. Marshall, I.M. Fishman, R.C. Dorfman, C.B. Eom, M.D. Fayer, Phys. Rev. 45B (1992) 10009.
[24] S. Sainov, J. Chem. Phys. 104 (1996) 6901.
[25] M. Terazima, Y. Kojima, N. Hirota, Chem. Phys. Lett. 259 (1996) 451.
[26] K. Ohta, M. Terazima, N. Hirota, Bull. Chem. Soc. Japan 68 (1995) 2809.
[27] M. Terazima, K. Okamoto, N. Hirota, J. Phys. Chem. 97 (1993) 5188.
[28] M. Terazima, Bull. Chem. Soc. Japan 69 (1996) 1881.
[29] J.A. Lee, T.P. Lodge, J. Phys. Chem. 91 (1987) 5546.
[30] D.J. Miles Jr., P.D. Lamb, K.W. Rhee, C.S. Johnson Jr., J. Phys. Chem. 87 (1983) 4815.
[31] J. Crank, The Mathematics of Diffusion, Oxford, New York, 1975.
[32] C.H. Wang, J.L. Xia, J. Phys. Chem. 96 (1992) 190.
[33] M. Misawa, T. Fukunaga, J. Chem. Phys. 93 (1990) 3495.
[34] W.D. Dozier, J.M. Drake, J. Klafter, Phys. Rev. Lett. 56 (1986) 197.
[35] J.C. Lee, J. Chem. Phys. 108 (1998) 2265.
[36] F. D'Orazio, S. Bhattacharja, W.P. Halperin, K. Eguchi, T. Mizusaki, Phys. Rev. B 42 (1990) 9810.
[37] T. Okazaki, N. Hirota, M. Terazima, J. Photochem. Photobiol. A 99 (1996) 155.
[38] G.H. Brown (Ed.), Photochromism, Wiley-Interscience, New York, 1971.
[39] H. Dürr, H. Bouas-Laurent (Ed.), Photochromism, Elsevier, New York, 1990.